Pediatric nasal epithelial cells are less permissive to SARS-CoV-2 replication compared to adult cells

Yanshan Zhu[1], Keng Yih Chew[1], Anjana C. Karawita[1], Ayaho Yamamoto[2], Larisa L. Labzin[3], Tejasri Yarlagadda[4], Alexander A. Khromykh[1,5], Claudia J. Stocks[3], Yao Xia[6], Tobias R. Kollmann[7], David Martino[7], Anthony Kicic[7,8,9], Merja Joensuu[10,11], Frédéric A. Meunier[10,11], Giuseppe Balistreri[11,12] Helle Bielefeldt-Ohmann[1,5,13], Asha C. Bowen[7,13], Peter D. Sly[2,14], Kirsten M. Spann[4], Kirsty R. Short[1,5*]

1 School of Chemistry and Molecular Biosciences, The University of Queensland, Brisbane, Australia
2 Child Health Research Centre, The University of Queensland, South Brisbane, QLD 4101, Australia
3 Institute for Molecular Bioscience, The University of Queensland, Brisbane, Australia
4 Centre for Immunology and Infection Control, Faculty of Health, School of Biomedical Sciences, Queensland University of Technology, Brisbane Queensland 4000, Australia
5 Australian Infectious Diseases Research Centre, Global Virus Network Centre of Excellence, Brisbane, Australia
6 School of Science, Edith Cowan University; School of Biomedical Science, The University of Western Australia, Perth, Australia
7 Wal-yan Respiratory Research Centre, Telethon Kids Institute, The University of Western Australia, Perth, Australia
8. Occupation and Environment, School of Public Health, Curtin University, Perth, Australia
9. Centre for Cell Therapy and Regenerative Medicine, School of Medicine and Pharmacology, The University of Western Australia, Perth, Australia
10. Clem Jones Centre for Ageing Dementia Research, Queensland Brain Institute, The University of Queensland, Brisbane, QLD, Australia.
11. Queensland Brain Institute, The University of Queensland, Brisbane, QLD, Australia.
12 Department of Virology, Faculty of Medicine, University of Helsinki, Finland
13 School of Veterinary Science, The University of Queensland, Gatton, Australia
14 Department of Infectious Diseases, Perth Children's Hospital, Nedlands, Perth, Western Australia

***Corresponding author:**
Kirsty R. Short, Ph.D., School of Chemistry and Molecular Biosciences, University of Queensland, Brisbane Australia
Phone: +61 7 336 54226; Email: k.short@uq.edu.au

Abstract

Children typically experience more mild symptoms of COVID-19 when compared to adults. There is a strong body of evidence that children are also be less susceptible to SARS-CoV-2 infection with the original Wuhan isolate. The reasons for reduced SARS-CoV-2 symptoms and infection in children remain unclear and may be influenced by a multitude of factors, including differences in target cell susceptibility and innate immune responses. Here, we use primary nasal epithelial cells from children and adults, differentiated at an air-liquid interface to show that SARS-CoV-2 (both the Wuhan isolate and the more recent Alpha variant) replicates to significantly lower titers in the nasal epithelial cells of children compared to those of adults. This was associated with a heightened antiviral response to SARS-CoV-2 in the nasal epithelial cells of children. Importantly, influenza virus, a virus whose transmission is frequently associated with pediatric infections, replicated in both adult and paediatric nasal epithelial cells to comparable titres. Taken together, these data show that the nasal epithelium of children supports lower infection and replication of SARS-CoV-2 than the adult nasal epithelium.

Keywords: SARS-CoV-2; pediatric nasal epithelial cells; anti-viral response; innate immune response; susceptibility to SARS-CoV-2 infection, alpha variant

INTRODUCTION

Severe Acute Respiratory Syndrome-Coronavirus 2 (SARS-CoV-2), the causative agent of coronavirus disease-2019 (COVID-19), causes a broad range of clinical symptoms, ranging from asymptomatic infection to potentially fatal acute respiratory distress syndrome (ARDS). Children typically experience mild symptoms of COVID-19 when compared to adults [1]. There is also a significant body of evidence with the original Wuhan SARS-CoV-2 isolate that children are less susceptible to SARS-CoV-2 infection and less likely to transmit the virus. Specifically, a low rate of pediatric SARS-CoV-2 infections has been observed in multiple countries including China [2], Italy [3], the U.S.A [4], Spain [5] and Poland [6]. Similarly, in a meta-analysis of SARS-CoV-2 household transmission clusters early in the pandemic, children were significantly less likely to contract SARS-CoV-2 from infected family members compared to adult members of the household [7]. These findings have been echoed in multiple single site studies where, both within and outside of households, the infection rate of SARS-CoV-2 amongst children <10 years old is significantly lower than that of adults [8]. Reduced SARS-CoV-2 infection and transmission is also observed in juvenile ferrets compared to their older counterparts [9].

In the second year of the SARS-CoV-2 pandemic numerous viral variants have become prevalent, including the Alpha variant (B.1.1.7) which contains multiple mutations in the spike protein, the N protein and various open reading frames (ORFs) of the virus. The SARS-CoV-2 Alpha variant is of significant concern because of its increased transmissibility and possible increased virulence[10]. Early evidence suggests that the Alpha variant, similarly to original Wuhan isolate, is associated with low risk of severe disease in young children[11,12]. Some studies have suggested that children are more susceptible to the Alpha variant compared to the original Wuhan isolate[13] whilst others have found little evidence of differential susceptibility[14].

The reduced susceptibility of children to SARS-CoV-2 infection and disease (at least some instances) is in stark contrast to other seasonal respiratory viruses, such as influenza virus, where children are thought to play a major role in the spread of the virus [15]. The reasons for less frequent SARS-CoV-2 infection and symptoms in children, at least with the original Wuhan isolate, remain unclear and may be influenced by a multitude of factors. Pre-existing immunity to SARS-CoV-2 (likely derived from seasonal coronaviruses) may offer some form of cross-protection from infection in children[16]. Indeed, SARS-CoV-2 spike glycoprotein reactive antibodies in uninfected individuals are more prevalent amongst children and adolescents [16].

It is also possible that nasal epithelial cells (NECs), the first site of infection, are fundamentally different in children compared to adults. Gene expression studies using the nasal epithelium of healthy individuals suggests that the transcript for the SARS-CoV-2 receptor, angiotensin

converting enzyme-2 (*ACE2*), is expressed at lower levels in children compared to adults [17]. However, this has yet to be validated on a protein level. Moreover, this does not appear to be the case in all patient cohorts [18,19]. Following binding of the SARS-CoV-2 spike protein to ACE2, the host surface transmembrane serine protease 2 (TMPRSS2) is also involved in viral entry into the cell [20]. NECS from children express less *TMPRSS2* mRNA than those from adults, which may contribute to less frequent pediatric infections with SARS-CoV-2 [21]. However, this has also yet to be confirmed at protein level.

In addition to differential receptor expression, pediatric and adult NECs may also mount fundamentally different innate immune response to SARS-CoV-2. Recent RNA sequencing of the whole epithelium from pediatric and adult proximal airways suggests that there is a higher expression of genes associated with inflammation and the anti-viral response in children compared to adults [22,23]. Whilst increased inflammation and interferon production have previously been associated with elevated COVID-19 severity [24], it is important to note that such studies refer to the inflammatory response in the lower respiratory tract, where any immunopathology may lead to respiratory distress [25]. In contrast, inflammation in the upper respiratory tract plays an important role in controlling early viral replication. Consistent with this supposition, nasopharyngeal swabs from SARS-CoV-2 infected children display elevated levels of interferons and inflammatory markers compared to those of SARS-CoV-2 infected adults [18]. However, whether this results in reduced replication of SARS-CoV-2 in the nasal epithelium of children remains to be determined.

Here, we use primary nasal epithelial cells (NECs), differentiated at an air-liquid interface, to investigate differential infection kinetics and antiviral responses to SARS-CoV-2 infection in children and adults.

METHODS

Cell collection and ethics statement

Primary NECs were collected from healthy adult (aged 21 to 65 years old) donors by placing a sterile nasal mucosal curette (Arlington Scientific Inc., USA) in the mid-inferior portion of the inferior turbinate during June 2020 to May 2021. Informed consent was obtained from all donors. Primary NECs were obtained from healthy pediatric donors (aged 2 to 7 years old) in the same manner while under general anesthetic prior to elective surgery for sleep apnoea or tonsilitis in 2019. Children did not have any other unknown underlying condition. A total of 10 adult donors and 12 pediatric donors were used for this study. This study was approved bythe University of Queensland's Human Research Ethics Committee (2020001742), the Queensland Children's Hospital and Health Service Human Research Ethics Committee (HREC/16/QRCH/215) and Queensland University of Technology Human Research Ethics Committee 17000000039). Primary NECs were stored in freezing media (FBS with 10% DMSO) after the second passage in culture.

Cell culture

African green monkey kidney epithelial Vero cells were maintained in MEM (Invitrogen), containing 10% (v/v) heat-inactivated fetal bovine serum (Cytiva), 100 U/ml penicillin and streptomycin (Life Technologies Australia). Madin-Darby Canine Kidney (MDCK) cells were maintained in DMEM (Invitrogen), containing 10% (v/v) heat-inactivated fetal bovine serum (Cytiva), 100 U/ml penicillin and streptomycin (Life Technologies Australia). All cell lines were obtained from American Type Culture Collection (ATCC; Virginia, USA). Primary NECs were expanded and passaged in Pneumacult EX Plus media (STEMCELL Technologies Inc, Canada). After initial expansion, NECs were seeded at a density of 4-5×10^5 cells/transwell on 6.5 mm transwell polyester membranes with 0.4um pores (Corning Costar, USA) and cultured in EX Plus media (STEMCELL Technologies). Cells were monitored for confluence. When a confluent monolayer was achieved, cells were 'air-lifted' by removing the media from the apical chamber and replacing the basolateral media with Pneumacult air liquid interface (ALI) media (STEMCELL Technologies) [26]. Medium was replaced in the basal compartment three times a week, and the cells were maintained in ALI conditions for at least 3 weeks until ciliated cells and mucus were observed and cells obtained a transepithelial electrical resistance (TEER) measurement greater than 1000Ω. Fully differentiated cultures were used in downstream infection experiments using influenza virus or SARS-CoV-2.

Viral stocks

SARS-CoV-2 isolate hCoV-19/Australia/QLD02/2020 (QLD02) (used as the original Wuhan isolate) and hCoV-19/Australia/QLD1517/2020(QLD1517) (GISAID accession EPI_ISL_944644; Alpha variant) were kindly provided by Queensland Health Forensic & Scientific Services, Queensland Department of Health. Virus was amplified in Vero cells

expressing human TMPRSS2 and titrated by plaque assay [27]. All studies with SARS-CoV-2 were performed under physical containment 3 (PC3) conditions and were approved by the University of Queensland Biosafety Committee (IBC/374B/SCMB/2020). A/Auckland/4/2009(H1N1) (Auckland/09) stocks were prepared in embryonated chicken eggs as previously described [28]. Viral titers were determined by plaque assays on MDCK cells, as previously described [29].

Viral infection

Differentiate adult and pediatric NECs were infected with mock (PBS), QLD02 (1.25 x 10^5 PFU), QLD1517 (2.4 x 10^4 PFU) or Auckland/09 (1.25 x 10^5 PFU). Specifically, 100uL of virus or PBS was placed on the epithelial surface in the apical compartment and incubated for 1 hour at 37ºC. Following incubation, excess virus was removed from the transwell and cells were incubated at 37ºC with 5% CO_2. Every 24 hours the basolateral media was refreshed with 1mL of new ALI media. At pre-determined timepoints post-infection 100µL of PBS (or in the case of influenza virus PBS + 0.1µg of TPCK-treated trypsin (Worthington, USA)) was added to the apical compartment and cells were incubated at 37ºC with 5% CO_2 for 10 minutes. The apical supernatant was subsequently removed and stored at -80ºC. Cells were lysed with Buffer RLT (Qiagen, USA) containing 0.01% β-mercaptoethanol for RNA analysis. Alternatively, cells were lysed in 2% SDS/PBS lysis buffer (2% SDS/PBS buffer, 10% 10x PhosSTOP, 4% 25x protease inhibitor) for protein analysis or fixed overnight in 4% paraformaldehyde for histology.

Histology

Fixed cells on a transwell membrane were routine processed and embedded in paraffin, sectioned at 5µm and subsequently stained with hematoxylin and eosin (H&E) or Periodic acid–Schiff (PAS). Sections were assessed for cellular morphology by a veterinary pathologist (H.B.O.) blinded to the experimental design.

Immunofluorescence

Differentiated epithelial cells grown on a transwell membrane were fixed with 4% paraformaldehyde (Cat#15710, Electron Microscopy Sciences) in PBS for 45 minutes at room temperature, followed by a blocking with 0.5% BSA (Sigma) in PBS for 30 minutes and permeabilization with 0.02% of Triton X-100 (Sigma) in PBS for 15 min at room temperature. After washing twice with PBS/BSA and a second blocking step for 10 min at room temperature, samples were incubated with primary antibodies overnight at 4°C. Primary antibodies were diluted in 0.5% BSA in PBS blocking solution: 1:400 ZO-1 (Cat#40-2200, Thermo Fisher Scientific); 1:1000 MUC5AC (Cat#MA5-12178, ThermoFisher Scientific); 1:500 ACE2 (Cat#AF933, R&D Systems). After three washing steps with 0.5% BSA/PBS for 5 minutes each time, the samples were incubated in secondary antibody: 1:1000 Alexa Flour 555 donkey

anti-goat (Cat#A21432, Invitrogen) for 2.5 hours at room temperature in dark, and after three washes in PBS and three washes with 0.5% BSA/PBS, the cells were incubated with a 1:1000 Alexa Fluor 647 goat anti-mouse (Cat#A32728, Invitrogen) for 2.5 hours at room temperature covered from light. The cells were simultaneously stained with 1:400 Alexa Fluor 647 Phalloidin (Cat#A22287 Invitrogen) and 1:1000 DAPI. After three washes in PBS, the transwell membranes with cells were cut with a scalpel, briefly dipped in milli-q water, and mounted on a class slide using ProLong Gold Antifade Mountant (Cat# P10144, ThermoFisher Scientific). Mounted samples were imaged on a spinning-disk confocal system (Marianas; 3I, Inc.) consisting of a Axio Observer Z1 (Carl Zeiss) equipped with a CSU-W1 spinning-disk head (Yokogawa Corporation of America), ORCA-Flash4.0 v2 sCMOS camera (Hamamatsu Photonics), and 63x 1.4 NA / Plan-Apochromat / 180 µm WD objective. Image acquisition was performed using SlideBook 6.0 (3I, Inc). 150 optical sections from five random regions of interest (ROIs) from each sample were acquired from the top of the differentiated epithelial cells. Image processing was performed using Fiji/ImageJ (Version 2.1.0/1.53c) as follows: Background was reduced using the Substract Backgound 50 pixel rolling ball radius, and the mean fluorescence intensity (MFI, a.u. arbitrary units) was measured from the average intensity images.

Western Blot

For total cell lysates, cells were washed twice with cold PBS and lysed with 2% SDS/PBS lysis buffer (2% SDS/PBS buffer, 10% 10x PhosSTOP, 4% 25x protease inhibitor). Pierce BCA protein assay kit (Thermo Fisher Scientific) was used to equalize protein amounts and SDS-sample buffer containing 100 mM DTT (Astral Scientific) was added. Samples were boiled at 100°C for 10 minutes to denature proteins. Proteins were separated on 4-15% mini protean TGX precast gels (Biorad) in running buffer (200 mM Glycine, 25 mM Tris, 0.1% SDS, pH8.6), transferred to nitrocellulose membrane (Cat#1620112, BioRad) in blot buffer (48 nM Tris, 39 nM Glycine, 0.04% SDS, 20% MeOH) and subsequently blocked with 5% (w/v) BSA in Tris-buffered saline with Tween 20 (TBST) for 30 minutes. The immunoblots were analyzed using primary antibodies incubated overnight at 4°C and secondary antibodies linked to horseradish peroxidase (HRP) (Invitrogen), and after each step immunoblots were washed 4x with TBST. HRP signals were visualized by enhanced chemiluminescence (ECL) (BioRad) and imaged with a Chemidoc (BioRad). Primary antibodies include GAPDH (14C10) Rabbit monoclonal antibody (1:2500 dilution, Cat#2118, Cell Signaling Technology), rabbit anti-SARS-CoV-2 Nucleoprotein/NP antibody (1:1000 dilution, Cat#40143-R040, Sino Biological), goat polyclonal ACE2 (1:500 dilution, Cat#AF933, R&D Systems), rabbit anti-TMPRSS2 antibody (1:1000 dilution, Cat#ab109131, Abcam). ImageJ was used to quantify the protein expression level relative to GAPDH levels.

Quantification of infectious virus

SARS-CoV-2 titers in cell culture supernatants were determined by plaque assay on Vero cells, as described previously [27]. Influenza virus titers in cell culture supernatants were determined by plaque assay on MDCK cells [29].

RNA extraction and quantitative Reverse Transcription PCR (qRT-PCR)

RNA was extracted from NECs using Nucleozole reagent according to the manufacturer's instructions, DNA was removed by DNase I (Thermo Fisher Scientific) treatment and 1 µg DNA-free RNA was reverse transcribed into cDNA using the High Capacity cDNA Reverse Transcription Kit (Applied Biosystems) on a Mastercycler Thermocycler (Eppendorf, Hamburg, Germany) according to the manufacturer's instructions using random primers. Real-time PCR was performed on generated cDNA with SYBER Green (Invitrogen) using QuantStudio 6 Flex Real-Time PCR System, an Applied Biosystems Real-Time PCR Instruments (Thermo Fisher Scientific). Gene expression was normalized relative to glyceraldehyde 3-phosphate dehydrogenase (*GAPDH*) expression, fold change was calculated using the ΔΔCt method. All primers used in this study are listed in Table 1.

Table 1. Primers used in the present study

Primer name	Sequence (5'-3')
h*IFIT1*	FW:TTGCCTGGATGTATTACCAC
	RV: GCTTCTTGCAAATGTTCTCC
h*CXCL10*	FW: GTGGCATTCAAGGAGTACCTC
	RV: GCCTTCGATTCTGGATTCAGACA
h*ISG15*	FW: GAGAGGCAGCGAACTCATCT;
	RV: CTTCAGCTCTGACACCGACA)
h*GAPDH*	FW: CGAGATCCCTCCAAAATCAA;
	RV: TTCACACCCATGACGAACAT

RNA Sequencing

RNA-Seq libraries were prepared using the Illumina stranded total RNA prep ligation with the Ribo-Zero plus kit (Illumina) and IDT for Illumina RNA UD Indexes according to the standard manufacturer's protocol. Briefly, 50ng of total RNA was depleted of rRNA and then fragmented by heat. cDNA was synthesized from the fragmented RNA using random primers. The first strand cDNA was converted into dsDNA in the presence of dUTP to maintain the 'strandedness' of the library. The 3' ends of the cDNA were adenylated and pre-index anchors were ligated. The libraries were then amplified with 14-16 cycles of PCR incorporating unique indexes for each sample to produce libraries ready for sequencing. The libraries were quantified on the Perkin Elmer LabChip GX Touch with the DNA High Sensitivity Reagent kit (Perkin Elmer). Libraries were pooled in equimolar ratios, and the pool was quantified by qPCR using

the KAPA Library Quantification Kit - illumina/Universal (KAPA Biosystems) in combination with the Life Technologies Viia 7 real time PCR instrument.

Sequencing was performed using the Illumina NextSeq500 (NextSeq control software v2.2.0 / Real Time Analysis v2.4.11). The library pool was diluted and denatured according to the standard NextSeq protocol and sequenced to generate single-end 76 bp reads using a 75 cycle NextSeq500/550 High Output reagent Kit v2.5 (Illumina). After sequencing, fastq files were generated using bcl2fastq2 (v2.20.0.422), which included trimming the first cycle of the insert read. Library preparation and sequencing was performed at the Institute for Molecular Bioscience Sequencing Facility (University of Queensland).

RNA Sequencing analysis

The quality of the trimmed RNA-seq reads was assessed with FastQC[30] and MultiQC[31]. Salmon[32] was used for transcript quantification from human transcriptome (GENCODE Release 36, accessed in December 2020). A decoy aware transcriptome file was created for Salmon transcript quantification followed by the transcriptome index[32]. The R package, DESeq2[33] was then used for differential gene expression (DGE) analysis and further validated through using the limma R package [34]with Voom transformation[35]. DGEs between virus and mock infected samples were analyzed by controlling the effect of the age group and gender of the individual samples, genes with adjusted *p*-value less than 0.05 were considered significant. Gene set enrichment analysis was performed using the R package GOseq[36.] All the R scripts were run on R-Studio platform (RStudio Team 2020, v 1.4.1717).

Code and data availability

RNA-seq data is deposited at European Nucleotide Archive under the project– PRJEB43102. The scripts used for RNA-seq data analysis including differential gene expression and gene set enrichment analysis can be found in https://github.com/akaraw/Yanshan_Zhu_et_al.

Statistical analysis

Where sufficient cell numbers were present, samples were performed in duplicate, and the results were averaged and shown as a single data point. If sufficient cells were not present, a single transwell was used to determine the response of that donor to viral infection. Data were tested for normality using the Shapiro-Wilk test. Outliers of continual variables were removed using ROUT's test (Q = 1%). Where data were normally distributed, data was analyzed using an unpaired two-tailed student's t-test. Where data were not normally distributed, data was analyzed using a Mann-Whitney U test. Significance was set at $p<0.05$.

RESULTS

Pediatric nasal epithelial cells are phenotypically different to adult nasal epithelial cells

To investigate the role of NECs in SARS-CoV-2 infection, adult and pediatric NECs were differentiated at an air-liquid interface. The phenotype of these cells at baseline (i.e., prior to infection) was then assessed. Adult NECs grew as a pseudostratified columnar epithelium with scattered goblet cells and ciliated epithelial cells (Figure 1A). Pediatric NECs also grew as a pseudostratified columnar epithelium with ciliated epithelial cells and goblet cells (Figure 1A). However, scattered cells with pyknotic nucleus and condensed cytoplasm were also observed, leaving pseudocysts in the epithelium (Supplementary Figure 1). This is potentially indicative of higher cell turn-over and metabolic rate in the pediatric epithelial cells [37,38]. Immunofluorescence images of zonal occludens-1 (ZO-1) stained NECs show that tight junction proteins were built up closely towards the apical region of both adult and pediatric cells (Figure 1B). PAS staining indicated the presence of mucus producing cells (Figure 1A) in both pediatric and adult NECs. Consistent with these data, MUC5AC staining was detected exclusively on the apical layer, thus demonstrating mucus secretion by differentiated NECs (Figure 1B).

Previous mRNA expression studies suggest that pediatric NECs express lower levels of *ACE2* and *TMPRSS2* compared to their adult counterparts [17,21]. However, these findings are inconsistent between patient cohorts and have not been investigated at a protein level [19]. Immunofluorescence staining suggested that pediatric NECs had lower surface levels of ACE2 compared to their adult counterparts (Figure 1B) although a limited sample size precluded statistical analysis (Figure 1C). Accordingly, we sought to confirm these data using western blot on the NECs from a larger number of donors (n = 5) (Figure 1D). Whilst the same trend was observed by western blot (increased levels of ACE2 in adult NECs) this failed to reach statistical significance (Figure 1D). There was no observable trend in TMPRSS2 levels between adult and pediatric NECs (Figure 1D).

Pediatric nasal epithelial cells are less permissive to SARS-CoV-2 replication

We next sought to determine if pediatric NECs were less susceptible than adult NECs to SARS-COV-2 (QLD02) replication. Strikingly, significantly reduced SARS-CoV-2 replication was observed in pediatric NECs at 24- and 72-hours post-infection (h.p.i) (Figure 2A). Reduced SARS-CoV-2 N protein level was also observed in pediatric NECs at 72 h.p.i, although this did not reach statistical significance ($p = 0.07$; Figure 2B and C, Supplementary Figure 2).To determine if decreased viral replication was specific to SARS-CoV-2, these experiments were repeated using influenza A virus, which is one of the many respiratory viruses known to be highly transmissible amongst children [39]. No significant difference in influenza A virus replication in pediatric NECs compared to adult cells was observed at 24-, 48- and 72-hour post-infection (Figure 2D).

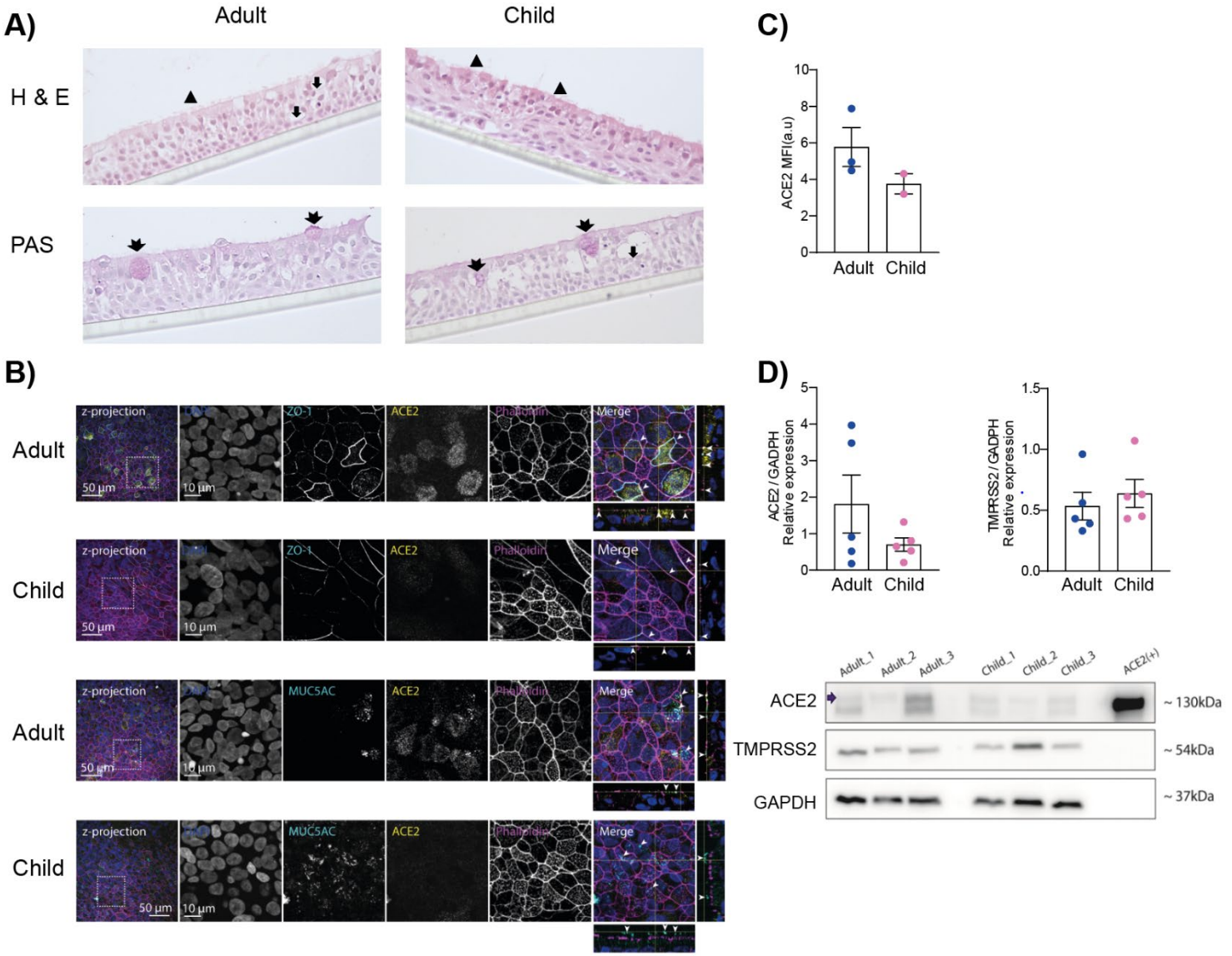

Figure 1. Pediatric nasal epithelial cells are phenotypically different to adult nasal epithelial cells. **A)** Representative H&E and PAS-stained sections of pediatric and adult NECs culture differentiated at an air-liquid interface (representative of 2 adult (1 female, 1 male) and 3 pediatric donors (1 female, 2 males)). Arrowheads indicate ciliated cells, arrows indicate goblet cells and double-tailed arrows indicate mucus producing cells as determined by PAS staining. Images taken at 400x magnification. **B)** Representative z-projections (150 optical sections) of pediatric and adult NECs cultures differentiated at an air-liquid interface and immunolabelled against endogenous ZO-1 and ACE2 (cyan and yellow, respectively, top panels), and MUC5AC and ACE2 (cyan and yellow, respectively, bottom panels). Cells were also stained with DAPI (blue) and phalloidin (magenta) to indicate the nucleus and actin filaments, respectively. The area in the dotted box in the images on left are shown magnified in the respective rows (10 µm bar applies to all images in the row). The merged image on right shows the orthogonal view of the z-stacks. The arrowheads indicate the zonal occludens-1 (ZO-1) stained profiles (top panels) and mucus secretion (MUC5AC) in the lower panels. **C)** Quantification of ACE2 immunofluorescence as described in the Materials and Methods. Mean ± SEM is shown. Each data point represents the average of five separate images taken from one

donor (pediatric (1 female, 1 male) and adult (2 females, 1 male) donor). **D)** Relative ACE2 and TMPRSS2 protein levels compared to GAPDH in pediatric (3 females, 2 males) and adult (4 females, 1 male) NECs. Each data point represents a different donor. Mean ± SEM is shown. C) Representative western blot of NECs from three adult and three pediatric donors blotted for ACE2, TMPRSS2 and GAPDH. ACE2 is indicated with an arrow.

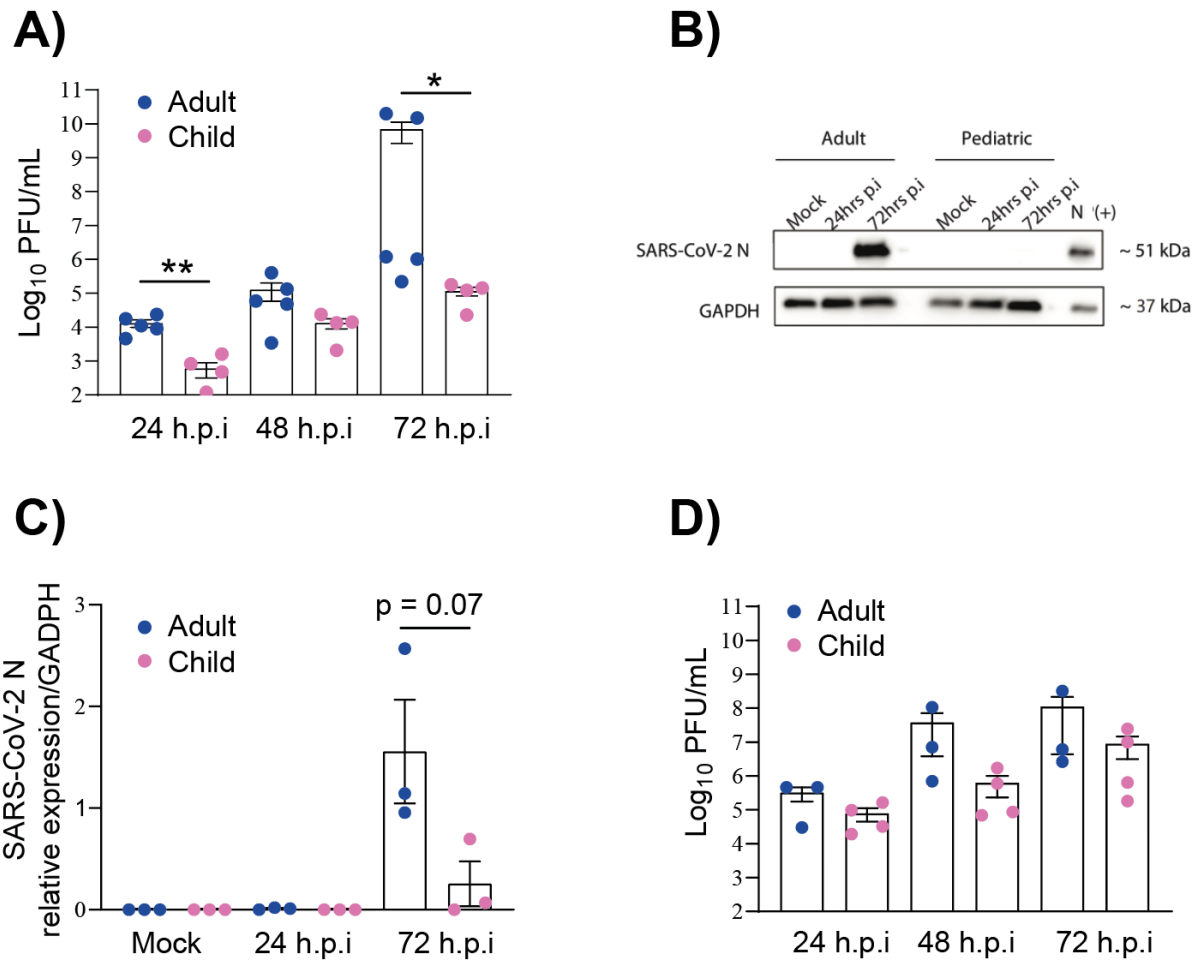

Figure 2. Lower replication of SARS-CoV-2 in pediatric nasal epithelial cells. **A**) Plaque forming units (PFU) of SARS-CoV-2 (QLD02) from the apical surface of nasal epithelial cells NECs obtained at 24, 48 and 72 h.p.i. **B**) Representative western blot of adult and pediatric donor blotted for SARS-CoV-2 N at various timepoints post-infection. All the western blot results (n= 3 adults and n = 3 children) for SARS-CoV-2 N are shown as Supplementary Figure 2. **C**) Relative SARS-CoV-2 N levels compared to GAPDH in pediatric and adult NECs. **D**) Plaque forming units (PFU) of influenza A virus from the apical surface of NECs at various timepoints post-infection. Each data point represents a separate donor. Mean ± SEM is shown. p <0.05*, p <0.01**. Statistical analysis performed as described in the Materials and Methods.

Pediatric nasal epithelial cells mount a strong anti-viral response to SARS-CoV-2

To gain a further insight into the observed decrease of SARS-CoV-2 replication in pediatric NECs RNA Seq was performed on infected adult and pediatric cells 72 hours post-SARS-CoV-2 (QLD02) infection. PCA analysis showed that infected cells formed distinct clusters depending on whether they were derived from pediatric or adult donors (Figure 3A). Numerous differentially genes were recorded in infected cells (Figure 3B). In infected pediatric NECs, gene ontology (GO) enrichment analysis (Figure 3C) demonstrated a strong interferon response, with GO terms such as 'viral process', 'type I interferon signaling', 'response to virus', 'regulation of defense response to virus', 'negative regulation of viral genome replication', 'defense response to virus' and 'cellular response to interferon alpha'. None of these GO terms were identified amongst the top differentially expressed GO terms in adult cells infected with SARS-CoV-2 (Figure 3D). In contrast, GO terms such as 'cellular response to sterol', 'Wnt signalling pathway' and 'response to tumor necrosis factor' were recorded. To confirm that these data were not restricted to a DESeq2 analysis, gene expression data were also analyzed using limma (Table 2 & 3). Once again, in infected pediatric NECs GO terms such as 'response to virus', 'cellular response to cytokine stimulus' and 'defense response to virus' were recorded (Table 2). In contrast, infected adult NECs were associated with GO terms such as 'detection of stimulus involved in sensory perception' and 'sensory perception' (Table 3). To further validate these data, we assessed gene expression by qPCR of three genes associated with inflammatory/anti-viral response - interferon-induced protein with tetratricopeptide repeats 1 (*IFIT1*); C-X-C motif chemokine ligand 10 (*CXCL10*) and interferon stimulated gene 15 (*ISG15*). Consistent with our RNA Seq data, infected pediatric NECs had significantly higher levels of *IFIT1* and *ISG15* compared to infected adult NECs (Figure 4A). Interestingly, these data were not restricted to SARS-CoV-2 infection and a similar expression profile was observed following influenza A virus infection (Figure 4B).

It has been suggested that children may be more susceptible to the recent SARS-CoV-2 variants of concern (VOC) compared to the original SARS-CoV-2 isolate. To determine if our findings were restricted to the parental Wuhan isolate, we infected pediatric and adult NECs with the Alpha variant (QLD1517). Consistent with our previous data we observed increased viral replication in adult NECs compared to those derived from pediatric donors (Figure 5A). This differential replication was associated with a differential expression of key interferon associated genes (Figure 5B).

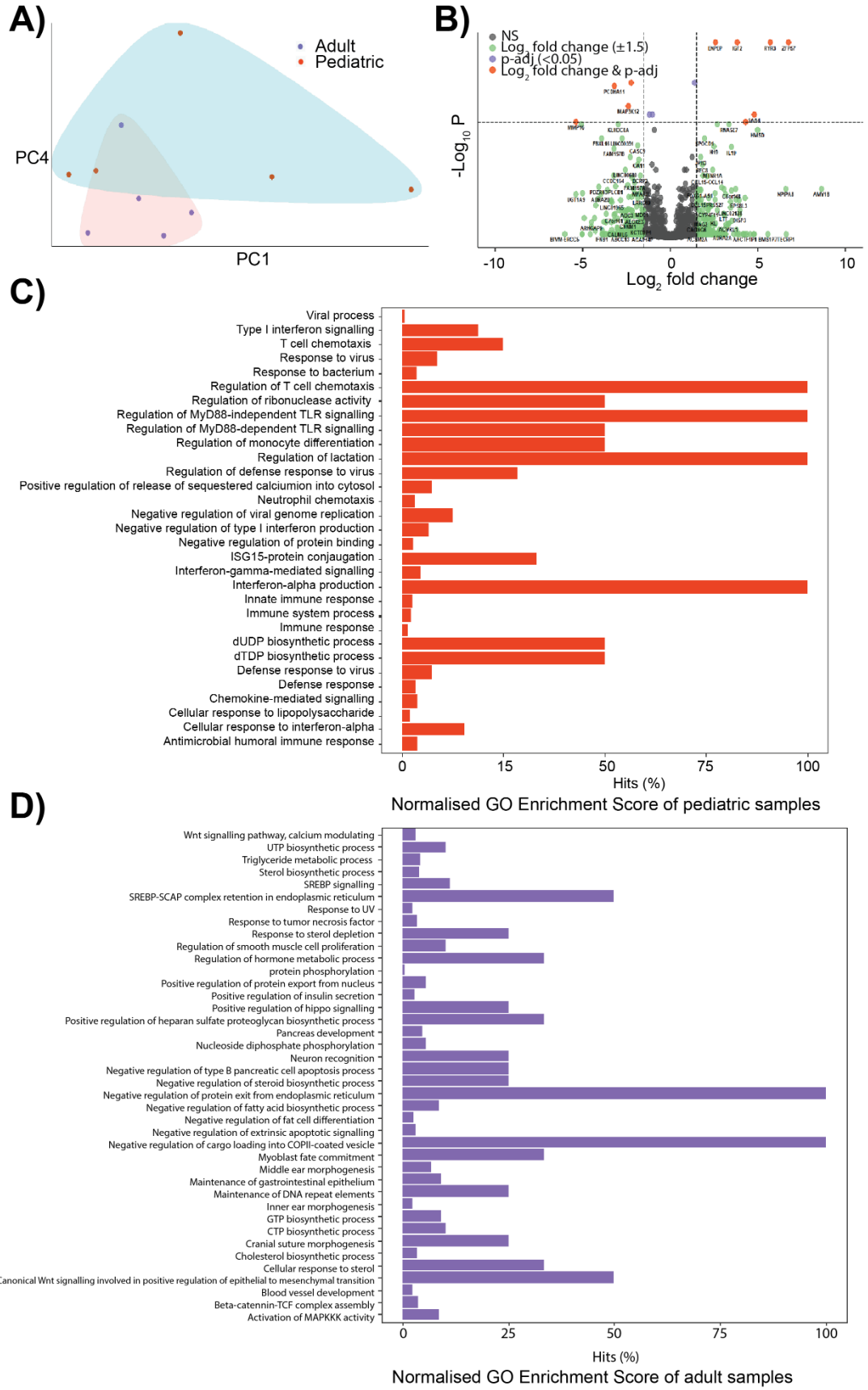

Figure 3: Pediatric epithelial cells have a different transcriptional response to SARS-CoV-2. A) Principal component analysis for the global transcriptional response of naive pediatric and adult NECs. Data points represent individual donors. **B)** Volcano plot illustrating differentially expressed genes (DEGs) of naive pediatric NECs compared to adult cells. DEGs statistically different between the two patient groups with a fold change of >1.5 are indicated in orange. DEGs statistically different between two groups with a fold change of <1.5 are shown in purple. DEGs not statistically different between two groups with a fold change of >1.5 are shown in green. NS = not significant. **C**) Gene ontology (GO) analysis of DEGs in infected pediatric NECs were displayed by the bar chart. The bars of significantly GO enriched (Overrepresented p value < 0.05) results were marked in red, x-axis reflects the gene count hits as a percentage over genes in each GO category; y-axis reflects different GO terms. **D)** Gene ontology (GO) analysis of DEGs in adult NECs were displayed by the bar chart. The bars of significantly enriched GO (Overrepresented p value < 0.05) enrichment results were marked in purple and represents the gene count hits (as a percentage over number of genes in a given category); y-axis reflects different GO terms.

Table 2: Significantly enriched gene ontology (Overrepresented *p value* < 0.05) terms in SARS-CoV-2 infected pediatric cells (relative to naïve cells)

	Term
GO:0071345	cellular response to cytokine stimulus
GO:0019221	cytokine−mediated signaling pathway
GO:0007166	cell surface receptor signaling pathway
GO:0009615	response to virus
GO:0007165	signal transduction
GO:0034097	response to cytokine
GO:0051607	defense response to virus
GO:0008219	cell death
GO:0012501	programmed cell death
GO:0065008	regulation of biological quality

Table 3: Significantly enriched gene ontology (Overrepresented *p value < 0.05*) terms in SARS-CoV-2 infected adult cells (relative to naïve cells)

	Term
GO:0050907	Detection of chemical stimulus involved in sensory perception
GO:0050906	detection of stimulus involved in sensory perception
GO:0009593	detection of chemical stimulus
GO:0007606	sensory perception of chemical stimulus
GO:0051606	detection of stimulus
GO:0050911	detection of chemical stimulus involved in sensory perception of smell
GO:0007186	G protein-coupled receptor signaling pathway
GO:0007608	Sensory perception of smell
GO:0007600	sensory perception
GO:0003008	system process
GO:0050877	nervous system process
GO:0002027	regulation of heart rate
GO:0003015	heart process
GO:0060047	heart contraction
GO:0008016	regulation of heart contraction
GO:0006805	xenobiotic metabolic process
GO:0001580	detection of chemical stimulus involved in sensory perception of bitter taste
GO:0050912	detection of chemical stimulus involved in sensory perception of taste
GO:0050913	sensory perception of bitter taste
GO:0007187	G protein−coupled receptor signaling

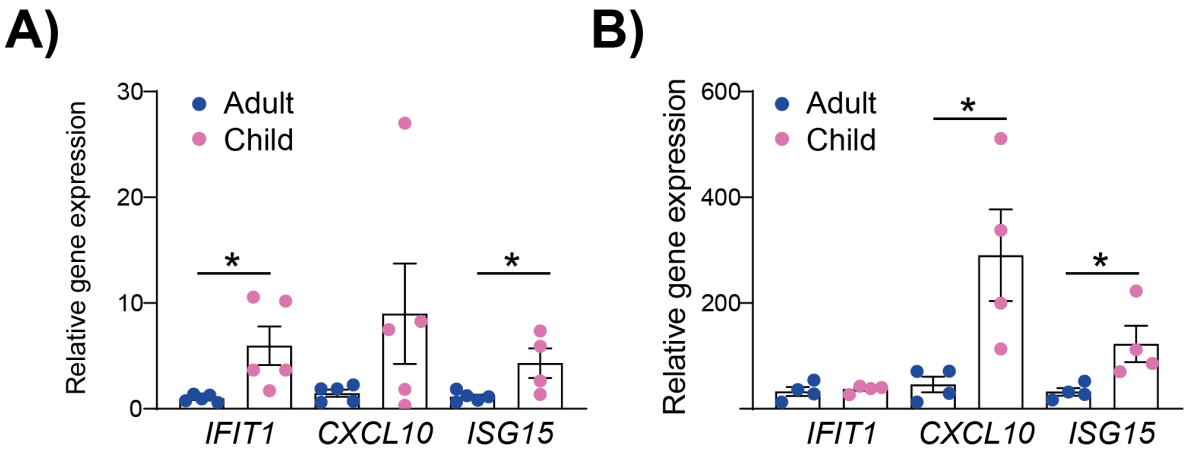

Figure 4: Pediatric epithelial cells have a stronger type I IFN response to viral infection. **A)** Expression of interferon associated genes in SARS-CoV-2 (QLD02) infected epithelial cells relative to uninfected controls (48 hours post-infection). **B)** Expression of interferon associated genes in influenza A virus infected epithelial cells relative to uninfected controls (48 hours post-infection). Each data point represents a different donor. Gene expression (fold change) was calculated using the ΔΔCt method relative to GAPDH expression. Mean ± SEM is shown. p <0.05*, statistical analysis performed as described in the Materials and Methods.

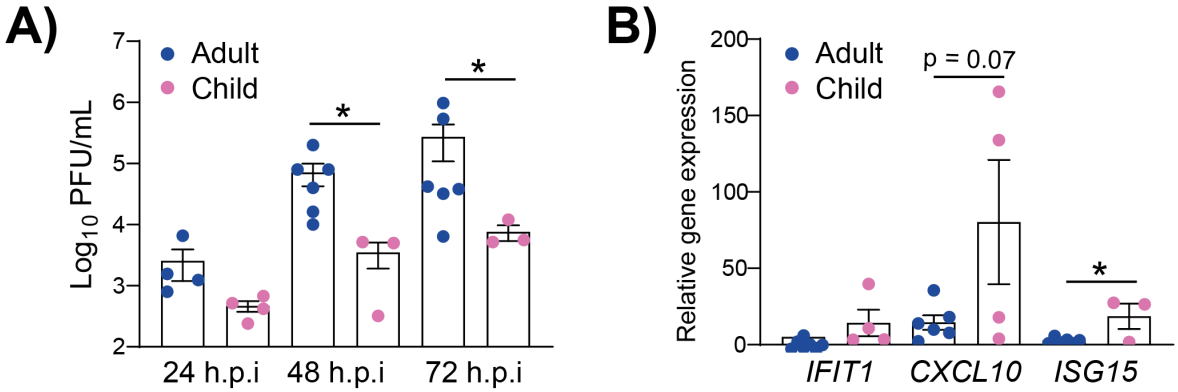

Figure 5. Lower replication of SARS-CoV-2 Alpha variant in pediatric nasal epithelial cells. **A**) Plaque forming units (PFU) of SARS-CoV-2 from the apical surface of nasal epithelial cells NECs obtained at 24, 48 and 72 h.p.i. **B)** Expression of interferon associated genes in influenza A virus infected epithelial cells relative to uninfected controls (48 h.p.i). Each data point represents a different donor. Gene expression (fold change) was calculated using the ΔΔCt method relative to GAPDH expression. Mean ± SEM is shown. p <0.05*. Statistical analysis performed as described in the Materials and Methods.

DISCUSSION

Large clinical data sets and systematic reviews suggest that children are less often infected and symptomatic with SARS-CoV-2 than adults [7,40-42]. However, the mechanisms driving these observations have been unclear. Here, we have provided the first experimental evidence that the pediatric nasal epithelium may play an important role in reducing the susceptibility of children to SARS-CoV-2 infection.

Previous studies have suggested that the reduced susceptibility of children to SARS-CoV-2 infection is due to reduced expression of ACE2 and TMPRSS2 mRNA. Specifically, it has been hypothesized that the lower level of ACE2 and TMPRSS2 in pediatric upper airways epithelial cells limits viral infectivity in children [17], although this has remained somewhat controversial [18,19]. In the present study, whilst there was a trend towards decreased ACE2 protein levels in pediatric NECs there was significant donor-to-donor variability that precluded statistical significance. We interpret these data as suggesting that ACE2 levels may contribute to, but are not the sole factor, in the increased resistance of children to SARS-CoV-2.

Despite donor-to-donor differences in ACE2 expression, we consistently observed a significant reduction in SARS-CoV-2 (QLD02) replication in pediatric NECs compared to NECs of adults. Given that the nasal epithelium is the first site of SARS-CoV-2 infection these data are consistent with the reduced number of SARS-CoV-2 infected children recorded in epidemiological studies [43,44]. There have been previous suggestions that nasopharyngeal SARS-CoV-2 titers in children and adolescents are equivalent to those of adults [45-47]. However, reanalysis of the aforementioned studies has shown that young children (<10 years old) did indeed have a significantly lower viral load [48], or that the comparison was being performed between children in the first 2 days of symptoms and hospitalized adults with severe disease [49] or that the dataset included few children younger than 16 years [50]. Indeed, it is challenging to compare data from controlled experimental studies to data obtained from patient sampling, where it is difficult to control for time of sampling relative to the onset of infection. Rather, decreased viral replication in pediatric epithelial cells is consistent with experimental studies in ferrets where aged ferrets showed higher viral load and longer nasal virus shedding [51].

Consistent with reduced SARS-CoV-2 replication in the nasal epithelium of children, pediatric epithelial cells had a more pronounced pro-inflammatory response (compared to adult cells) following a SARS-CoV-2 infection. In particular, a pronounced interferon response and the expression of interferon stimulated genes (*ISGs*) was higher in infected pediatric, compared to adult, NECs. Increased *ISG* expression, and the subsequent anti-viral response may contribute to the reduced viral replication observed in pediatric cells. Importantly, unlike the lower respiratory tract, any resultant cell death or immunopathology in the upper respiratory tract is unlikely to lead to respiratory distress and therefore remains beneficial to the host [24]. These

findings are consistent with those of Maughan et al, who analyzed transcriptional profile of airway (tracheobronchial) epithelium and observed upregulated type I and II *IFNs* associated genes in children [23]. Similarly, in the nasal fluid of children and adults presenting to the emergency department with SARS-CoV-2 there were significantly higher levels of *IFN-α2* in the fluid derived from children. Increased interferon signaling was also recorded in the nasopharyngeal transcriptome of children compared to that of adults during early SARS-CoV-2 infection [18,22]. The question remains as to why pediatric epithelial cells mount a stronger inflammatory and anti-viral response to SARS-CoV-2 compared to adult cells. This may represent an adaptation to the increased antigenic challenge observed in childhood. Alternatively, it is possible that increased antigenic exposure in childhood 'trains' nasal epithelium in children to mount a stronger pro-inflammatory response to any antigenic challenge. It is also possible that metabolic differences between pediatric and NECs (as potentially suggested by the different morphologies of the cells) could alter gene expression. It is also important to recognize that these data may not be applicable to all patient populations as previous studies of children and adults hospitalized with COVID-19 did not find an age-dependent difference in the interferon response [52].

A pronounced pro-inflammatory and anti-viral response in pediatric cells was not restricted to SARS-CoV-2 infection and a similar result was observed following influenza virus infection. However, influenza virus replicated equally as well in pediatric cells compared to adults. These data are consistent with the high sensitivity of children to influenza virus infection [39]. These data are also seemingly discordant with the increased interferon response of pediatric cells. However, SARS-CoV-2 is highly sensitive to interferon treatment, more so than influenza A virus [53,54]. Therefore, we speculate that whilst the differential interferon response between children and adults is sufficient to inhibit SARS-CoV-2 replication, it is not sufficient to inhibit influenza virus replication.

The growing dominance of SARS-CoV-2 VOCs has raised speculation that the epidemiology of SARS-CoV-2 infection has fundamentally changed. Namely, there have been suggestions children are more susceptible to VOCs compared to the original Wuhan isolate [55]. This is difficult to discern using epidemiological data alone, as data are confounded by the fact that unlike adults, young children are not routinely vaccinated. The data presented here would suggest that the pediatric epithelium still confers some protection against the replication of the Alpha variant. Whether this remains true of other VOCs (including the more recent Delta variant), and in a more complex *in vivo* situation, remains to be determined.

Finally, it is important to recognize the limitations of this study. Due to the difficulties associated with obtaining NECs from children only a limited number of donors could be used for this study. However, as donors were not selected according to susceptibility to respiratory

viral infection, their responses should be broadly representative of healthy children. Furthermore, our data focused on the role of nasal epithelial cells in age-dependent differences in SARS-CoV-2 infection. However, there may be other mechanisms to explain the reduced susceptibility of children to SARS-CoV-2 infection that were not measured in the present study. For example, children and adolescents have much higher titers of preexisting antibodies to SARS-CoV-2 compared to adults [16]. This study is unable to ascertain if this plays a more significant role than the nasal epithelium in protecting children from infection *in vivo*. Finally, it is important to recognize that it is possible that the data presented herein were not the result of age differences between pediatric and adult NECs and were instead the result of another undefined factor that was also different between the two patient groups.

Despite these potential limitations, the data presented here strongly suggest that the nasal epithelium of children is distinct and that it may afford children some level of protection from SARS-CoV-2 infection.

Author Contributions:

The authors meet criteria for authorship as recommended by the International Committee of Medical Journal Editors, contributed to the manuscript and have given final approval for the version to be published. Y.Z. and K.R.S. wrote the manuscript. T.R.K, A.C.B., K.M.S. and K.R.S. designed the study, Y.Z., K.Y.C., A.Y., L.L, T.Y., A.A.K., C.J.S. and H.B.O. collected the data. Y.Z., K.Y.C., A.C.K., C.J.S., Y.X., D.M., A.K., M.J., G.B., F.A.M. and K.R.S. analyzed the data. Y.Z., A.C.K. M.J., G.B. and K.R.S. designed the figures. P.D.S. K.M.S. and K.R.S. recruited study participants. All authors approved the final manuscript.

Acknowledgments

We greatly thank the participants in the study and the members of the research team. We would also like to acknowledge health care providers and their families worldwide.

Funding

This work is supported by the Australia Research Council (Fellowship DE180100512 to K.R.S and Discovery Early Career Researcher Award DE190100565 to M.J.), The National Health and Medical Research Council (Project grant APP1139316 and Senior research Fellowship APP1155794 to F.A.M.), and Academy of Finland and COVID19 research donations (Grant 318434 to G.B.).

663 **SUPPLEMENTARY FIGURES:**
664

665
666 **Supplementary Figure 1: Pediatric nasal epithelial cells display pseudocysts**.
667 Representative Hematoxylin & Eosin-stained section of pediatric NECs culture differentiated
668 at an air-liquid interface.
669

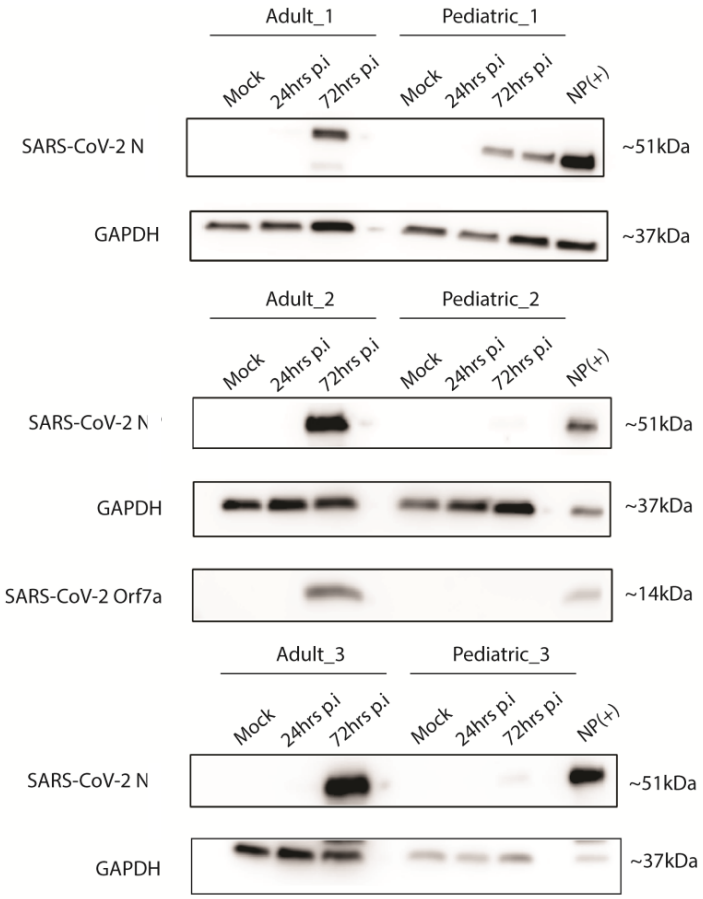

670
671

672 **Supplementary Figure 2. Relative SARS-CoV-2 NP levels compared to GAPDH in pediatric and**
673 **adult NECs.** Western blot of adults and pediatric donors blotted for SARS-CoV-2 N at various
674 timepoints post-infection (n=3 adults (2 females, 1 male) and n = 3 children (1 female, 2 males)).
675
676

677 # REFERENCES

678 1. Lu X, Zhang L, Du H, et al. SARS-CoV-2 Infection in Children. *New England Journal of Medicine*
679 2020; **382**(17): 1663-5.

680 2. Lee P-I, Hu Y-L, Chen P-Y, Huang Y-C, Hsueh P-R. Are children less susceptible to COVID-19? *J*
681 *Microbiol Immunol Infect* 2020; **53**(3): 371-2.

682 3. Lanari M, Chiereghin A, Biserni GB, Rocca A, Re MC, Lazzarotto T. Children and SARS-CoV-2
683 infection: innocent bystanders…until proven otherwise. *Clin Microbiol Infect* 2020; **26**(9): 1130-2.

684 4. Team CC-R. Coronavirus Disease 2019 in Children - United States, February 12-April 2, 2020.
685 *MMWR Morb Mortal Wkly Rep* 2020; **69**(14): 422-6.

686 5. Tagarro A, Epalza C, Santos M, et al. Screening and Severity of Coronavirus Disease 2019 (COVID-
687 19) in Children in Madrid, Spain. *JAMA Pediatr* 2021; **175**(3): 316-7.

688 6. Kuchar E, Załęski A, Wronowski M, et al. Children were less frequently infected with SARS-CoV-2
689 than adults during 2020 COVID-19 pandemic in Warsaw, Poland. *European Journal of Clinical*
690 *Microbiology & Infectious Diseases* 2021; **40**(3): 541–7.

691 7. Zhu Y, Bloxham CJ, Hulme KD, et al. A meta-analysis on the role of children in SARS-CoV-2 in
692 household transmission clusters. *Clin Infect Dis* 2020: ciaa1825.

693 8. Goldstein E, Lipsitch M, Cevik M. On the Effect of Age on the Transmission of SARS-CoV-2 in
694 Households, Schools, and the Community. *The Journal of Infectious Diseases* 2021; **223**(3): 362-9.

695 9. Hua C-Z, Miao Z-P, Zheng J-S, et al. Epidemiological features and viral shedding in children with
696 SARS-CoV-2 infection. *Journal of Medical Virology* 2020; **92**(11): 2804-12.

697 10. Khateeb J, Li Y, Zhang H. Emerging SARS-CoV-2 variants of concern and potential intervention
698 approaches. *Critical Care* 2021; **25**(1): 244.

699 11. Nyberg T, Twohig KA, Harris RJ, et al. Risk of hospital admission for patients with SARS-CoV-2
700 variant B.1.1.7: cohort analysis. *Bmj* 2021; **373**: n1412.

701 12. Somekh I, Sharabi A, Dory Y, Simões EAF, Somekh E. Intrafamilial Spread and Altered
702 Symptomatology of SARS-CoV-2, During Predominant Circulation of Lineage B.1.1.7 Variant in Israel.
703 *Pediatr Infect Dis J* 2021; **40**(8): e310-e1.

704 13. Ladhani SN, Ireland G, Baawuah F, et al. Emergence of SARS-CoV-2 Alpha (B.1.1.7) variant,
705 infection rates, antibody seroconversion and seroprevalence rates in secondary school students and
706 staff: active prospective surveillance, December 2020 to March 2021, England. *Journal of Infection*
707 2021.

14. Meyer M, Holfter A, Ruebsteck E, et al. The Alpha Variant (B.1.1.7) of SARS-CoV-2 in Children: First Experience from 3544 Nucleic Acid Amplification Tests in a Cohort of Children in Germany. *Viruses* 2021; **13**(8).

15. Longini IM, Jr., Koopman JS, Monto AS, Fox JP. Estimating household and community transmission parameters for influenza. *Am J Epidemiol* 1982; **115**(5): 736-51.

16. Ng KW, Faulkner N, Cornish GH, et al. Preexisting and de novo humoral immunity to SARS-CoV-2 in humans. *Science* 2020; **370**(6522): 1339-43.

17. Bunyavanich S, Do A, Vicencio A. Nasal Gene Expression of Angiotensin-Converting Enzyme 2 in Children and Adults. *JAMA* 2020; **323**(23): 2427-9.

18. Pierce CA, Sy S, Galen B, et al. Natural mucosal barriers and COVID-19 in children. *JCI Insight* 2021; **6**(9).

19. Wark PAB, Pathinayake PS, Kaiko G, et al. ACE2 expression is elevated in airway epithelial cells from older and male healthy individuals but reduced in asthma. *Respirology* 2021: doi: 10.1111/resp.14003.

20. Hoffmann M, Kleine-Weber H, Schroeder S, et al. SARS-CoV-2 Cell Entry Depends on ACE2 and TMPRSS2 and Is Blocked by a Clinically Proven Protease Inhibitor. *Cell* 2020; **181**(2): 271-80.e8.

21. Saheb Sharif-Askari N, Saheb Sharif-Askari F, Alabed M, et al. Airways Expression of SARS-CoV-2 Receptor, ACE2, and TMPRSS2 Is Lower in Children Than Adults and Increases with Smoking and COPD. *Molecular Therapy - Methods & Clinical Development* 2020; **18**: 1-6.

22. Loske J, Röhmel J, Lukassen S, et al. Pre-activated anti-viral innate immunity in the upper airways controls early SARS-CoV-2 infection in children. *medRxiv* 2021: 2021.06.24.21259087.

23. Maughan EF, Nigro E, Pennycuick A, et al. Cell-intrinsic differences between human airway epithelial cells from children and adults. *bioRxiv* 2020: 2020.04.20.027144.

24. Lucas C, Wong P, Klein J, et al. Longitudinal analyses reveal immunological misfiring in severe COVID-19. *Nature* 2020; **584**(7821): 463-9.

25. Short KR, Kroeze EJBV, Fouchier RAM, Kuiken T. Pathogenesis of influenza-induced acute respiratory distress syndrome. *The Lancet Infectious Diseases* 2014; **14**(1): 57-69.

26. Hou YJ, Okuda K, Edwards CE, et al. SARS-CoV-2 Reverse Genetics Reveals a Variable Infection Gradient in the Respiratory Tract. *Cell* 2020; **182**(2): 429-46.e14.

27. Gordon DE, Jang GM, Bouhaddou M, et al. A SARS-CoV-2 protein interaction map reveals targets for drug repurposing. *Nature* 2020; **583**(7816): 459-68.

739 28. Short KR, Diavatopoulos DA, Reading PC, et al. Using bioluminescent imaging to investigate
740 synergism between Streptococcus pneumoniae and influenza A virus in infant mice. *J Vis Exp* 2011;
741 (50).

742 29. Siegers JY, Novakovic B, Hulme KD, et al. A High-Fat Diet Increases Influenza A Virus-Associated
743 Cardiovascular Damage. *The Journal of Infectious Diseases* 2020; **222**(5): 820-31.

744 30. S A. FastQC: a quality control tool for high throughput sequence data. Available online at:
745 http://www.bioinformatics.babraham.ac.uk/projects/fastqc). 2020.

746 31. Ewels P, Magnusson M, Lundin S, Käller M. MultiQC: summarize analysis results for multiple
747 tools and samples in a single report. *Bioinformatics* 2016; **32**(19): 3047-8.

748 32. Patro R, Duggal G, Love MI, Irizarry RA, Kingsford C. Salmon provides fast and bias-aware
749 quantification of transcript expression. *Nat Methods* 2017; **14**(4): 417-9.

750 33. Love MI, Huber W, Anders S. Moderated estimation of fold change and dispersion for RNA-seq
751 data with DESeq2. *Genome Biol* 2014; **15**(12): 550.

752 34. Ritchie ME, Phipson B, Wu D, et al. limma powers differential expression analyses for RNA-
753 sequencing and microarray studies. *Nucleic Acids Res* 2015; **43**(7): e47.

754 35. Law CW, Chen Y, Shi W, Smyth GK. voom: Precision weights unlock linear model analysis tools
755 for RNA-seq read counts. *Genome Biol* 2014; **15**(2): R29.

756 36. Young MD, Wakefield MJ, Smyth GK, Oshlack A. Gene ontology analysis for RNA-seq: accounting
757 for selection bias. *Genome Biology* 2010; **11**(2): R14.

758 37. Bardanzellu F, Fanos V. How could metabolomics change pediatric health? *Italian Journal of*
759 *Pediatrics* 2020; **46**(1): 37.

760 38. Yazicioglu T, Mühlfeld C, Autilio C, et al. Aging impairs alveolar epithelial type II cell function in
761 acute lung injury. *Am J Physiol Lung Cell Mol Physiol* 2020; **319**(5): L755-l69.

762 39. Kondrich J, Rosenthal M. Influenza in children. *Curr Opin Pediatr* 2017; **29**(3): 297-302.

763 40. Lachassinne E, de Pontual L, Caseris M, et al. SARS-CoV-2 transmission among children and staff
764 in daycare centres during a nationwide lockdown in France: a cross-sectional, multicentre,
765 seroprevalence study. *Lancet Child Adolesc Health* 2021.

766 41. Stringhini S, Wisniak A, Piumatti G, et al. Seroprevalence of anti-SARS-CoV-2 IgG antibodies in
767 Geneva, Switzerland (SEROCoV-POP): a population-based study. *Lancet* 2020; **396**(10247): 313-9.

768 42. Tönshoff B, Müller B, Elling R, et al. Prevalence of SARS-CoV-2 Infection in Children and Their
769 Parents in Southwest Germany. *JAMA Pediatrics* 2021.

770 43. Mehta NS, Mytton OT, Mullins EWS, et al. SARS-CoV-2 (COVID-19): What Do We Know About
771 Children? A Systematic Review. *Clin Infect Dis* 2020; **71**(9): 2469-79.

772 44. Zimmermann P, Curtis N. Why is COVID-19 less severe in children? A review of the proposed
773 mechanisms underlying the age-related difference in severity of SARS-CoV-2 infections. *Archives of*
774 *Disease in Childhood* 2020: archdischild-2020-320338.

775 45. Baggio S, L'Huillier AG, Yerly S, et al. SARS-CoV-2 viral load in the upper respiratory tract of
776 children and adults with early acute COVID-19. *Clin Infect Dis* 2020.

777 46. Chung E, Chow EJ, Wilcox NC, et al. Comparison of Symptoms and RNA Levels in Children and
778 Adults With SARS-CoV-2 Infection in the Community Setting. *JAMA Pediatr* 2021.

779 47. Jacot D, Greub G, Jaton K, Opota O. Viral load of SARS-CoV-2 across patients and compared to
780 other respiratory viruses. *Microbes Infect* 2020; **22**(10): 617-21.

781 48. Li X, Xu W, Dozier M, He Y, Kirolos A, Theodoratou E. The role of children in transmission of
782 SARS-CoV-2: A rapid review. *J Glob Health* 2020; **10**(1): 011101.

783 49. Yonker LM, Neilan AM, Bartsch Y, et al. Pediatric Severe Acute Respiratory Syndrome
784 Coronavirus 2 (SARS-CoV-2): Clinical Presentation, Infectivity, and Immune Responses. *J Pediatr* 2020;
785 **227**: 45-52.e5.

786 50. Singanayagam A, Patel M, Charlett A, et al. Duration of infectiousness and correlation with RT-
787 PCR cycle threshold values in cases of COVID-19, England, January to May 2020. *Euro Surveill* 2020;
788 **25**(32).

789 51. Young-Il K, Kwang-Min Y, June-Young K, et al. Age-dependent pathogenic characteristics of
790 SARS-CoV-2 infection in ferrets. *Research Square* 2021.

791 52. Koch CM, Prigge AD, Anekalla KR, et al. Immune response to SARS-CoV-2 in the nasal mucosa in
792 children and adults. *medRxiv* 2021: 2021.01.26.21250269.

793 53. Blanco-Melo D, Nilsson-Payant BE, Liu W-C, et al. Imbalanced Host Response to SARS-CoV-2
794 Drives Development of COVID-19. *Cell* 2020; **181**(5): 1036-45.e9.

795 54. Wu W, Metcalf JP. The Role of Type I IFNs in Influenza: Antiviral Superheroes or
796 Immunopathogenic Villains? *Journal of Innate Immunity* 2020; **12**(6): 437-47.

797 55. van Oosterhout C, Stephenson JF, Weimer B, Ly H, Hall N, Tyler KM. COVID-19 adaptive
798 evolution during the pandemic – Implications of new SARS-CoV-2 variants on public health policies.
799 *Virulence* 2021; **12**(1): 2013-6.

800